Published in final edited form as:
Development. 2008 December ; 135(23): 3891–3901. doi:10.1242/dev.029264.

Tailbud-derived Bmp4 drives proliferation and inhibits maturation of zebrafish chordamesoderm

Robert Esterberg, **Jean-Marie Delalande**, and **Andreas Fritz***
Department of Biology, Emory University, Atlanta, GA 30322, USA

Abstract

In zebrafish, BMP signaling establishes cell identity along the dorsoventral (DV) axis during gastrulation. Owing to the early requirements of BMP activity in DV patterning, it has been difficult to assign later roles in cell fate specification to specific BMP ligands. In this study, we have taken advantage of two *follistatin-like* genes (*fstl1* and *fstl2*), as well as a transgenic zebrafish line carrying an inducible truncated form of the BMP-type 1 receptor to study the role of Bmp4 outside of the context of DV specification. Characterization of *fstl1/2* suggests that they exert a redundant role as BMP antagonists during late gastrulation, regulating BMP activity in axial mesoderm. Maintenance of appropriate levels of BMP signaling is crucial for the proper development of chordamesoderm, a subset of axial mesoderm that gives rise to the notochord, but not prechordal mesoderm, which gives rise to the prechordal plate. Bmp4 activity in particular is required during a crucial window beginning at late gastrulation and lasting through early somitogenesis to promote chordamesoderm proliferation. In the absence of Bmp4, the notochord precursor pool is depleted, and the notochord differentiates prematurely. Our results illustrate a role for Bmp4 in the proliferation and timely differentiation of axial tissue after DV axis specification.

Keywords

Bmp4; Chordamesoderm; Notochord; Zebrafish

INTRODUCTION

In zebrafish, BMP signaling acts progressively during gastrulation to establish mesodermal cell identity. Mesoderm is specified early in gastrulation and contributes to tissues that can be roughly categorized as dorsal or ventral in nature. The specification of ventral fate involves Bmp2b/7 signaling and activation of downstream transcription factors such as SMAD1/5/8, *vent1*, *ved* and *vox* (Kimelman, 2006; Schier and Talbot, 2005; Yamamoto and Oelgeschlager, 2004). SMAD1/5/8 activity on the presumptive ventral side of the blastula activates the expression of ventral genes, whereas *vent1*, *ved* and *vox* repress the expression of genes that confer dorsal identity such as the BMP antagonist *chordin* (Imai et al., 2001; Kawahara et al., 2000; Melby et al., 2000). Establishment of the DV axis is followed by a second phase of BMP signaling during mid to late gastrulation, when the interaction of BMP antagonists and agonists is thought to establish a BMP activity gradient (Kimelman, 2006; Schier and Talbot, 2005). According to this model, high, intermediate and low levels of BMP activity in the mesoderm specify ventral, intermediate and dorsal fate, respectively.

*Author for correspondence (e-mail: afritz@emory.edu).

Supplementary material
Supplementary material for this article is available at http://dev.biologists.org/cgi/content/full/135/23/3891/DC1

Low levels of BMP activity direct cells surrounding the dorsal organizer to become axial mesoderm, whereas their positions within this tissue influence their exposure to other activity gradients (Schier and Talbot, 2005; Stemple, 2005). For example, Nodal activity is crucial for the process of further specification of axial mesoderm. High levels of Nodal, received by cells deep in the organizer, specify cells to become prechordal plate (Gritsman et al., 2000; Saude et al., 2000). Low levels of Nodal activity found in the superficial organizer specify cells to become chordamesoderm, the antecedent of the notochord (Gritsman et al., 2000; Saude et al., 2000).

The molecular events surrounding the transition of chordamesoderm into mature notochord are not fully understood, although there are several defining features of the process (Stemple, 2005). Differentiated notochord cells acquire large vacuoles that allow the tissue to provide structural support to the embryo. Coupled with this, genes expressed in chordamesoderm are extinguished as the tissue matures. These include the *sonic hedgehog* and *indian hedgehog* homologs, *shha* and *ihhb*, respectively, as well as the extracellular matrix (ECM) gene *collagen 2a* (*col2a1a*) (Currie and Ingham, 1996; Krauss et al., 1993; Yan et al., 1995). Mutagenesis screens and studies examining ECM members have begun to elucidate the chordamesodermal transition into mature notochord. Embryos lacking Laminin 1 subunits (*bashful*, *grumpy* and *sleepy*) (Parsons et al., 2002), Laminin α4/5 (Pollard et al., 2006) and Collagen15a1 (Pagnon-Minot et al., 2008) continue to express chordamesodermal markers after expression has been extinguished in wild-type embryos, suggesting that notochord differentiation is impaired. However, given their nature, these proteins are unlikely to play instructive roles in notochord differentiation. The signal responsible for promoting notochord development has yet to be defined.

Although it is clear that initial specification of chordamesoderm is reliant upon the absence of BMP from the dorsal organizer, subsequent proliferation and differentiation of this tissue may depend upon it. Posterior to the notochord lies the chordoneural hinge (CNH), a stem cell pool that contributes to notochord, floor plate and tailbud mesoderm (Cambray and Wilson, 2002; Cambray and Wilson, 2007; Charrier et al., 1999; Davis and Kirschner, 2000; Kanki and Ho, 1997). Several agonists of BMP activity, including the BMP ligand ADMP, are expressed in axial territories during gastrulation and in the CNH during segmentation stages (Dickmeis et al., 2001; Lele et al., 2001). Thus, BMP signaling may play an important role in the development of axial mesoderm after specification of the DV axis. However, the role of BMPs in DV establishment masks their later functions. For example, manipulation of ADMP levels within the embryo causes DV patterning phenotypes that are difficult to resolve from tissue-specific defects (Lele et al., 2001; Willot et al., 2002).

In contrast to the known role of BMP activity in DV establishment, prior studies have not addressed the role of the BMP activity gradient in relation to axial mesoderm. In this study, we have identified both a requirement for BMP activity in the development of this tissue, as well as the signaling molecule responsible for notochord differentiation. We have been able to address these issues through the inactivation of two BMP antagonists, *fstl1* and *fstl2* (Dal-Pra et al., 2006), that act redundantly to inhibit BMP activity beginning at late gastrulation. Inactivation of these genes, as well as of Bmp4 and BMP signaling, reveals that Bmp4 promotes the proliferative capacity of notochord and CNH cells. In the absence of Bmp4, chordamesoderm fails to proliferate and the notochord differentiates prematurely. Our results illustrate the requirement of *fstl1* and *fstl2* in late gastrulation to maintain proper BMP activity levels, which are necessary for the development and timely differentiation of dorsal structures.

MATERIALS AND METHODS

Heat-shock conditions

Tg(hsp70l:dnBmpr-GFP)^{w30} (*tBR*) transgenic zebrafish were obtained from the Kimelman laboratory (University of Washington, Seattle). This transgenic line contains a truncated Type I BMP receptor containing GFP in place of the kinase domain under the control of a heat shock promoter (Pyati et al., 2005). *tBR* embryos were heat-shocked at 37°C for 1 hour at the time indicated according to Pyati et al. (Pyati et al., 2005). Where appropriate, wild-type embryos were heat-shocked under the same conditions to serve as controls.

In situ hybridization

The following probes were used: *admp* (Lele et al., 2001), *bmp4* (Nikaido et al., 1997), *col2a1a* (Yan et al., 1995), *eve1* (Joly et al., 1993), *flh* (Talbot et al., 1995), *fstl1* (Dal-Pra et al., 2006), *fstl2* (Dal-Pra et al., 2006), *gsc* (Schulte-Merker et al., 1994), *ihhb* (Currie and Ingham, 1996), *ntl* (Schulte- Merker et al., 1992), *shha* (Krauss et al., 1993) and *spt* (Griffin et al., 1998).

mRNA synthesis

Full-length *fstl1/2* cDNA was cloned into pCS2+. Capped mRNAs were transcribed using RNA polymerase in vitro transcription kits (mMESSAGE mMACHINE; Ambion). Approximately 100 pg of *fstl1* or *fstl2* mRNA was injected into one- and two-cell stage embryos.

Morpholino injection

Translation-blocking morpholinos are overlap with 22 nucleotides at the 5′ end of the previously published MO sequence (Dal-Pra et al., 2006). *fstl1* and *fstl2* translation-blocking MOs were as follows: *fstl1*, 5′-GCAGCTGCATGGACAGAGTGAAAAC-3′; *fstl2*, 5′-CACGGGTAAACACCGAAACATCATT-3′. *fstl* splice-blocking morpholinos were as follows: *fstl1*, 5′-CAGACTTACCTTCACATTGTCCGTC-3′; *fstl2*, 5′-AAATTAAAGCTCACCATCACAAGTC-3′. To ensure MO function, RNA was isolated from injected embryos and RT-PCR was performed using primers designed around intron-exon boundaries. Those sequences are as follows: *fstl1*, 5′-TAATCATCCAGTCTGTGGCAGTAAT-3′ and 5′-CTTGGGCTGTTGATGAT-3′; *fstl2*, 5′-GGTCTGCACCGCCATGACTTGT-3′ and 5′-ACACGGCGGGTCCACTCCTC-3′. For single morpholino injections, 8 ng of MO were injected into one- and two-cell stage embryos. For double morpholino injections, ~6 ng of each MO was injected. The control morpholino sequence used was 5′-CCTCTTACCTCAGTTACAATTTATA-3′. Where appropriate, control MO was injected into embryos that were subsequently heat-shocked at 37°C for 1 hour. The *bmp4* splice-blocking morpholino used has been previously characterized (Chocron et al., 2007).

Antibody staining

Labeling with PSMAD1/5/8 was as previously described (Rentzsch et al., 2006). Labeling with Myf5 and F59 were as previously described (Hammond et al., 2007; Topczewska et al., 2001). The primary antibodies were against Myf5 (anti-Myf5 recognizes Myod1 in zebrafish; Santa Cruz, C-20) at 1:50, F59 (anti-MyHC; University of Iowa Developmental Studies Hybridoma Bank) at 1:10, 4D9 (anti-Engrailed; University of Iowa Developmental Studies Hybridoma Bank) at 1:20, Prox1 (Angiobio) at 1:500 and P-SMAD1/5/8 (Chemicon International) at 1:100. Alexa-conjugated Phalloidin (Molecular Probes) was used at a 1:50 dilution to label F-actin. Appropriate Alexa Fluor (Molecular Probes) secondary antibodies were used.

Western blots

Protein extracts were prepared using standard procedures (Westerfield, 1994). Anti-P SMAD1/5/8 and Anti-P SMAD2 (Cell Signaling Technology) were used at a concentration of 1:1000.

BrdU labeling

Twelve-somite embryos were incubated with a solution of 425 µl BrdU labeling reagent (Roche Applied Science) and 75 µl DMSO for 45 minutes at 6°C. They were then washed in embryo medium for 30 minutes at 28.5°C and fixed with 4% PFA in PBS. BrdU incorporated cells were detected using Alexa Fluor 594 goat anti-mouse IgG at 1:500.

Cell transplantation and margin extirpation

Surgical transplantation and extirpation experiments were performed as described (Saude et al., 2000). For ventral margin extirpation, ~100 cells were removed by suction from the ventral margin of 80% epiboly embryos. For cell transplantation, donor embryos were injected with a 5% solution of fluorescein dextran (10K MW; Molecular Probes) at one- and two-cell stage embryos. Approximately 30 ventral margin cells taken from shield-stage donors were transplanted into the dorsal organizer of an equivalently staged host. *tBR* embryos were obtained from an incross of homozygous *tBR* parents. Both donor and host embryo were then heat-shocked after transplantation to maximize BMP signaling inhibition according to previous transplantation protocols (Pyati et al., 2005).

Cell cycle inhibition

Published protocols were followed with slight modifications (Stern et al., 2005). Embryos were treated with a combination of 150 µM aphidicolin and 20 mM hydroxyurea in 4% DMSO between 80% epiboly and bud stage. Cell proliferation was assayed through BrdU incorporation at stages during and after application.

Bead implantation

Human Bmp2/7 and zebrafish Bmp4 protein-coated beads (R&D Systems) were prepared by overnight incubation of 45 µm polystyrene beads (Polysciences) in a 500 µg/ml solution of recombinant Bmp2/7 or Bmp4 protein (R&D Systems) in PBS. Before implantation, beads were rinsed three times for 10 minutes in PBS. Control beads were loaded with 500 µg/ml BSA.

Cell counting

DAPI-positive cells were quantified and compared by one-way ANOVA, followed by a two-tailed, equal variance *t*-test.

RESULTS

Two BMP antagonists redundantly antagonize BMP activity after DV axis specification

To explore the significance of BMP activity after the onset of gastrulation, we further characterized the roles of two previously identified *follistatin-like* genes (*fstl1* and *fstl2*) (Dal-Pra et al., 2006). These genes are structurally and functionally related to Follistatin (Fst), a known inhibitor of Bmp4 and ADMP (Dal-Pra et al., 2006; Dosch and Niehrs, 2000; Fainsod et al., 1997; Iemura et al., 1998). Although *fstl2* mRNA can be detected in cleavage-stage embryos, *fstl1* expression is initiated during late gastrulation in dorsal structures. Unlike *fst*, which is expressed only in anterior paraxial mesoderm (Bauer et al., 1998), *fstl1/2* share largely overlapping expression patterns throughout axial and paraxial mesoderm during late

gastrulation and segmentation stages (see Fig. S1 in the supplementary material) (see also Dal-Pra et al., 2006). Fstl2 plays a minor role in BMP antagonism during DV axis specification, as depletion of Fstl2 in a Chordin/Noggin1-deficient embryo slightly increases the severity of the ventralization phenotype observed in Chordin/Noggin1 double morphants. Loss of Fstl2 in either Chordin or Noggin1 single morphant embryos does not enhance the ventralization phenotype (Dal-Pra et al., 2006). As shown by these authors, we observed no DV patterning defects when either Fstl protein was reduced by itself or in combination with each other. The most pronounced morphological defect observed in Fstl1/2 morphants was an enlarged undulating notochord that became less prominent as somitogenesis continued (e.g. see Fig. S2 in the supplementary material; Fig 3 and Fig 6). In addition, we found an increase in the levels of molecular markers that indicated an increase in BMP activity (Fig 1 and Fig 2).

The domain of the tailbud, which is dependant on BMP activity (Holley, 2006; Szeto and Kimelman, 2006), was increased in Fstl morphant embryos and enlarged to a greater degree when Fstl1 and Fstl2 were knocked down in concert. The expression domain of *spadetail* (*spt*), a T-box domain transcription factor required for trunk segmental identity (Griffin et al., 1998), was increased in Fstl1/2 morphant embryos (Fig. 1A,B; see Fig. S2 in the supplementary material). The domain of expression of BMP agonists, which are positively regulated in response to BMP activity, was expanded in the tailbud in a similar fashion (Yamamoto and Oelgeschlager, 2004). This included the expression domains of *bmp4* and the transcriptional target of BMP activity, *eve1* (Fig. 1E,F,M,N; see Fig. S2 in the supplementary material) (Pyati et al., 2005), as well as *admp* in the posterior notochord (Fig. 1Q,R). We also observed an increase in phosphorylated (P) SMAD 1/5/8 in the tailbud, which is activated in response to BMP signaling (Fig. 1I,J) (Yamamoto and Oelgeschlager, 2004). Western blots against PSMAD1/5/8 indicated that BMP activity is increased in Fstl1/2 morphants beginning at late gastrulation. Prior to 80% epiboly, we observed no change in PSMAD1/5/8 levels (not shown). At the end of gastrulation, we observed an increase in BMP activity that was present at every stage assayed, through 18 somites (Fig. 1U). Follistatin also binds Activin ligands with high affinity, which initiates intracellular Nodal cascades (Harrington et al., 2006; Nakamura et al., 1991). We observed no change in PSMAD2 levels, a target of Nodal signaling (reviewed by Kitisin et al., 2007), in Fstl1/2 morphants at any stage assayed (Fig. 1U).

To assess morpholino specificity, we compared the phenotypes generated using non-overlapping translation- and splice-blocking morpholino sequences. The tailbud and notochord phenotypes observed using translation-blocking morpholinos were indistinguishable from those observed using splice-blocking morpholinos (see Fig. S2 in the supplementary material). In general, morphant phenotypes were reliable and were observed in greater than 90% of embryos (n>500). Furthermore, we attempted to rescue the tailbud phenotype observed in Fstl1/2 morphants. Injection of either *fstl1* or *fstl2* mRNA caused a reduction in the tailbud domain, consistent with a decrease in BMP activity and a role for Fstl1 and Fstl2 as BMP antagonists (Fig. 1C,G,K,O,S) (also data not shown). Co-injection of either *fstl1* or *fstl2* mRNA and *fstl1/2* morpholinos was sufficient to rescue the Fstl1/2 double morphant phenotype, demonstrating the specificity of our morpholinos and a functional redundancy between Fstl1 and Fstl2 (Fig. 1D,H,L,P,T) (also data not shown). As all of the morphant phenotypes were comparable with each other, the Fstl1/2 morphant phenotypes illustrated here are of embryos injected with *fstl1/2* splice-blocking morpholinos.

Bmp4 activity during late gastrulation is required for chordamesoderm patterning

The expression of *fstl1/2* along the dorsal midline and the notochord defects observed in *fstl1/2* morphants suggest a function in axial development. We observed no changes in the expression of axial markers in Fstl1/2 morphants until late gastrulation, consistent with the temporal rise in PSMAD1/5/8 levels. At 70% epiboly, *goosecoid* (*gsc*) expression in prechordal

mesoderm (Schulte-Merker et al., 1994) and *floating head* (*flh*), *no tail* (*ntl*) and *admp* expression in chordamesoderm (Dickmeis et al., 2001; Schulte-Merker et al., 1992; Talbot et al., 1995) of Fstl1/2 morphants were comparable with controls (Fig. 2A,B,H,I,O,P,V,W). At 90% epiboly, the domain of prechordal mesoderm was unchanged in Fstl1/2 morphant embryos (Fig. 2C,D), but the domain of chordamesoderm was expanded anteriorly (Fig. 2J,K,Q,R,X,Y).

As changes in chordamesodermal gene expression in Fstl1/2 morphants appeared to be a result of increased BMP activity, we wished to determine the effects of lowering BMP activity on this tissue. We were able to conditionally inactivate BMP activity through the use of a transgenic zebrafish line carrying a truncated BMP-type I receptor fused to GFP under the control of a heat-shock promoter (abbreviated *tBR*) (Pyati et al., 2005). Heat shocking these embryos for 1 hour at 37°C blocks BMP effector expression for at least 2 hours and is capable of inducing severe dorsalization phenotypes depending on the timing of heat shock (Pyati et al., 2005). To determine the temporal effectiveness of this transgene, *tBR* embryos were heat-shocked during late gastrulation in hourly intervals and stained with PSMAD1/5/8 antibodies (see Fig. S3 in the supplementary material). Between 1 and 3 hours post heatshock, PSMAD1/5/8-positive cells were not detectable in *tBR* embryos, suggesting that heatshock attenuates BMP activity over this time range during early somitogenesis.

As we observed an expanse in chordamesoderm and an increase in PSMAD1/5/8 levels during late gastrulation in Fstl1/2 morphants, we heat-shocked *tBR* embryos at 80% epiboly to examine the consequence of blocking BMP activity on chordamesoderm. In these embryos, the domain of prechordal mesoderm was unchanged relative to heat-shocked controls (Fig. 2E), whereas chordamesoderm was absent anteriorly (Fig. 2L,S,Z). Knockdown of Bmp4 also resulted in a reduction of chordamesoderm (Fig. 2M,T,AA), but not of prechordal mesoderm (Fig. 2F). The reduced domain of chordamesoderm observed when Fstl1, Fstl2 and Bmp4 were knocked down together resembled that of Bmp4 morphant embryos (Fig. 2N,U,BB).

A crucial window of Bmp4 activity establishes the proliferative state and size of the CNH and notochord

Using riboprobes against *shha* and *ntl*, we examined the effect of manipulating BMP activity on the size of the notochord and CNH. The size of the CNH in Fstl1/2 morphant embryos was expanded when compared with controls (Fig. 3A,B,K,L). Sections through the trunk between somites 5–10 revealed that the diameter of the notochord was also increased in these embryos; the mean number of cells populating the notochord was increased by 63% when compared with controls (Fig. 3F,G) (4.1 cells versus 6.5 cells, $n=10$; $P<0.001$).

In contrast to the expansion of the notochord and CNH observed in Fstl1/2 morphant embryos, attenuation of Bmp4 activity caused a reduction in both the diameter of the notochord as well as the size of the CNH. The axial phenotype observed when Bmp4 was knocked down largely resembled that of *tBR* embryos that were heat-shocked at 80% epiboly (Fig. 3C,E,M,O), with the mean number of cells populating the notochord decreased by ~41% (Fig. 3H,J) (4.1 cells versus 2.4 cells and 2.9 cells, $n=10$; $P<0.001$). The difference in notochord cells of *tBR* embryos and Bmp4 morphants was not significant ($P>0.05$). In both *tBR* embryos heat-shocked at 80% epiboly and Bmp4 morphants, we observed the formation of ectopic tail structures. These observations are consistent with roles assigned to BMP activity in patterning ventroposterior tissues during late gastrulation (Pyati et al., 2005; Stickney et al., 2007).

To determine the temporal requirements of axial cells for BMP activity, we heat-shocked *tBR* embryos at hourly intervals beginning at 80% gastrulation, corresponding to the time at which increased PSMAD1/5/8 levels were observed in Fstl1/2 morphants. The size of the notochord and CNH in embryos heat-shocked at bud stage was comparable to those of embryos heat-shocked at 80% epiboly (not shown). Embryos heat-shocked at the three-somite stage

yielded a notochord diameter and CNH domain that were indistinguishable from heat-shocked controls (Fig. 3D,I,N) (4.1 cells versus 4.3 cells, n=10; P>0.05).

We wished to address the underlying cause of the increase in chordamesoderm. Because chordamesoderm transfates to paraxial mesoderm in *flh* mutants (Halpern et al., 1995), we reasoned that an expanse in chordamesoderm may occur at the expense of paraxial mesoderm. However, the analysis of *deltaC* (*dlC*), *myod1* and *paraxial protocadherin* (*papc*) expression revealed no changes in paraxial territory of Fstl1/2 morphants or in *tBR* embryos heat-shocked at 80% epiboly (see Fig. S7 in the supplementary material) (also data not shown).

Because our results did not suggest that fate assignment was disrupted in Fstl1/2 morphants, we addressed whether the increase in chordamesoderm was due to increased cell proliferation by assaying BrdU incorporation. In 14-somite controls, we observed PSMAD1/5/8 and BrdU antibodies co-labeling notochord cells (Fig. 4A –A″)). In addition to labeling these cells in Fstl1/2 morphants, cells of the CNH were positive for PSMAD1/5/8 and BrdU, and axial cells that were BrdU-positive were also positive for PSMAD1/5/8 (Fig. 4B-B″). Axial cells of Fstl1/2 morphants that were BrdU positive were also found in positions more anterior than in controls (not shown). By contrast, heat-shocking *tBR* embryos at 80% epiboly or bud stage resulted in loss of BrdU incorporation in both endogenous and ectopic axial structures (Fig. 4C-C″) (also data not shown). We observed no changes in cell proliferation when we heat-shocked *tBR* embryos at the 3-somite stage (not shown). The presence of PSMAD1/5/8-positive axial cells in Bmp4 morphants (Fig. 4D-D″) indicates that axial cells receive signaling from multiple BMP ligands, and also that loss of Bmp4 does not affect signaling of other BMPs, consistent with previous reports (Stickney et al., 2007). Nevertheless, reduction of Bmp4 levels was sufficient to inhibit axial proliferation; cell proliferation in Bmp4 morphants resembled that of *tBR* embryos heat-shocked at 80% epiboly. This suggests that BMP activity, particularly Bmp4, acts prior to the 3-somite stage to promote chordamesodermal proliferation.

Ventral margin as the source of axially required BMP ligands

The ventral margin acts as the major secreting center of BMPs during gastrulation (Agathon et al., 2003; Schier and Talbot, 2005; Yamamoto and Oelgeschlager, 2004) and is in close proximity to dorsal cells at the end of gastrulation. However, because BMP signaling initiates positive-feedback mechanisms in target cells (Yamamoto and Oelgeschlager, 2004), an alternate source of BMP ligands might initiate from PSMAD1/5/8-positive chordamesoderm. To demonstrate that BMP signals originate from the ventral margin, we removed ~100 cells from the ventral side of the embryo at 80% epiboly and examined the effects on chordamesoderm. Embryos lacking most of their ventral margin resembled Bmp4 morphants; the sizes of ventral fin and ventral somitic mesoderm were reduced (see Fig. S4A in the supplementary material). Both the domain of chordamesoderm as well as cell proliferation in this tissue was reduced, resembling that of Bmp4 morphants and *tBR* embryos heat-shocked at 80% epiboly (see Fig. S4B–E″ in the supplementary material). This suggests that chordamesoderm possesses a requirement for ventrally derived BMP ligands during late gastrulation.

BMP activity levels influence the temporal state of the notochord

In addition to notochord size, we wished to determine whether alteration of BMP activity affects the timing of notochord differentiation. In both *tBR* embryos heat-shocked at 80% epiboly and Bmp4 morphants, the expression of markers indicative of chordamesoderm was shifted such that they resembled expression patterns seen in more mature notochord. At the 9-somite stage, expression of *ihhb*, which can be detected throughout the entire notochord in control embryos, was maintained only in the caudal notochord of embryos lacking Bmp4 (Fig. 5A–C). Likewise, *shha* expression was lost from the notochord but maintained in floor plate

and the diencephalon in 24 hpf *tBR* embryos, Bmp4 morphants and embryos lacking ventral margin (Fig. 5E–G,I–K; see Fig. S3G I the supplementary material). These results were confirmed by loss of *ptc1* expression from the trunk and tail, where the expression pattern of 24 hpf embryos lacking Bmp4 resembled 36 hpf controls (Fig. 5M–O,DD; see Fig. S4H in the supplementary material). *col2a1a* expression was absent from the floor plate of 36 hpf *tBR* embryos heat-shocked at 80% epiboly and Bmp4 morphants, and more closely resembled the expression observed in 48 hpf controls (Fig. 5Q–S,GG).

Conversely, in Fstl1/2 morphants, chordamesodermal gene expression was prolonged when compared with controls, resembling that of embryos at younger developmental stages. Expression of *ihhb*, which is restricted to the caudal notochord in 18-somite stage embryos, was maintained in the rostral notochord of Fstl1/2 morphant embryos (Fig. 5U,V). We also observed *shha* expression in vacuolated notochord cells and *ptc1* expression in axial and paraxial tissues of the trunk of 36 hpf Fstl1/2 morphants, where they are not expressed in controls (Fig. 5X,Y,AA,BB,DD,EE). *col2a1a* expression was maintained in the notochord of 48 hpf Fstl1/2 morphants (Fig. 5GG,HH), resembling expression of 24 hpf controls (Yan et al., 1995). The gene expression patterns observed in Fstl1/2 morphants are consistent with a delay in transitioning into differentiated notochord, as is observed in embryos lacking Col15a1 (Pagnon-Minot et al., 2008) and Laminin1/4/5 (Parsons et al., 2002; Pollard et al., 2006).

As cells populating the notochord become vacuolated during differentiation, we examined the morphology of the notochord in embryos with altered BMP activity. In 24 hpf controls, notochord cells swell and become vacuolated in an anterior to posterior fashion (Fig. 6A,C,D). Although we did not observe any changes in anterior cell morphology at the level of the hind yolk extension in Fstl1/2 morphants, cells of the caudal notochord at the level of the cloaca were smaller than those observed in control embryos (Fig. 6B,E,F). Conversely, *tBR* embryos heat-shocked at 80% epiboly and Bmp4 morphants exhibited caudal notochord cells at the level of the cloaca that became vacuolated well before those observed in control embryos (Fig. 6G–J). Precocious vacuolation of notochord cells was also observed in embryos lacking ventral margin (see Fig. S4F in the supplementary material). This suggests that prolonged BMP activity delays the chordamesodermal transition into mature notochord. In the absence of Bmp4, the notochord differentiates prematurely.

The proliferative state of chordamesoderm establishes the timing of notochord maturation

Alterations in BMP activity levels influence both the proliferative properties of chordamesoderm, as well as the timing of its differentiation. To determine whether the proliferative capacity of chordamesoderm influences the timing of its maturation, we used small molecule inhibitors of the cell cycle (Stern et al., 2005) to block cell proliferation during the window in which BMP activity influences the proliferative capacity of chordamesoderm. We found that treating embryos from 80% epiboly to bud stage with a combination of hydroxyurea and aphidicolin effectively blocked cell proliferation during late gastrulation (see Fig. S5A,B in the supplementary material) (also data not shown). Removing the inhibitors at bud stage allowed proliferation to resume 2 hours after washing, although BrdU incorporating cells were not observed in chordamesoderm (see Fig. S5C-C″ in the supplementary material). The chordamesoderm defects observed in embryos treated with cell cycle inhibitors during late gastrulation resembled the defects observed in embryos lacking Bmp4. Expression of the chordamesodermal markers *ihhb*, *shha* and *col2a1a* resembled expression in Bmp4 morphants (Fig. 5D,H,L,P,T), and notochord cells at the level of the cloaca became vacuolated before those of controls (Fig. 6K,L).

In contrast to embryos with reduced BMP activity, chordamesoderm proliferation is increased and transition into mature notochord is delayed in Fstl1/2 morphants. By treating Fstl1/2 morphants with hydroxyurea and aphidicolin from 80% epiboly to bud stage, we were able to

rescue the prolonged expression of chordamesoderm markers. Expression of *ihhb* and *shha* was restricted to caudal notochord in these embryos, resembling comparably staged controls (Fig. 5W,Z,CC). Similarly, *col2a1a* expression was lost from the notochord and floor plate of 48 hpf Fstl1/2 morphants treated with cell cycle inhibitors, also resembling controls (Fig. 5II). This suggests that the proliferative state of chordamesoderm, which is established during late gastrulation, determines the timing of the chordamesoderm transition into mature notochord.

A direct role for BMP signaling in notochord development

The presence of PSMAD1/5/8-positive cells (Fig. 4) suggests that chordamesoderm is directly influenced by BMP activity. To demonstrate that this tissue autonomously responds to BMP signaling, we removed ~30 cells from the ventral margin of shield stage embryos and transplanted them into the dorsal organizer of an equivalently staged host (Fig. 6O). Upon placing wild-type cells into a wild-type host, these cells reliably populated the notochord, consistent with previous fate mapping and transplantation studies (Gritsman et al., 2000;Saude et al., 2000). Transplantation of ventral wild-type cells into *tBR* embryos heat-shocked after transplantation resulted in donor cell morphology resembling that of control embryos (94/132) (Fig. 6P,Q). Surprisingly, we found that these cells populated the entire notochord at the exclusion of endogenous *tBR* cells. Following the transplantation of ventral *tBR* cells into wild-type embryos, the *tBR* cells consistently failed to populate the notochord (0/151) (Fig. 6R,S). They did, however, populate adjacent paraxial mesoderm, contributing to myofibers and somitic cells. Thus, BMP activity biases cells in proximity of the dorsal organizer to become chordamesoderm.

To further explore the effects of Bmp4 activity on notochord fate, recombinant zebrafish Bmp4-soaked beads were implanted near the organizer of shield-stage embryos (Fig. 7A). This way, involuting cells would be exposed to Bmp4. Embryos exposed to ectopic Bmp4 exhibited an expanse of chordamesoderm at late gastrulation stages and an increase in notochord and CNH size in segmentation stage embryos when compared with embryos exposed to BSA-soaked beads (Fig. 7B,C,J,K). At 24 hpf, the notochord of these embryos was composed of a bilayer of cells rather than a monolayer observed in controls, and development of the floor plate was delayed (Fig. 7D,F,G,I). By 48 hpf, the floor plate became visible in Bmp4-treated embryos, although notochord cell morphology remained irregular (Fig. 7M,N). These cells did not fully vacuolate, and some cells remained arranged in a bilayer. *tBR* embryos exposed to Bmp4-soaked beads and heat-shocked at 80% epiboly did not exhibit enlarged notochords (Fig. 7E,H).

Because we observed that axial cells remained PSMAD1/5/8-positive when Bmp4 was knocked down, we wished to examine the effects of other BMPs on notochord development (see Fig. S6 in the supplementary material). Implantation of beads soaked with recombinant human Bmp2/7 did not noticeably alter the domain of chordamesoderm or notochord morphology when compared with controls.

The timing of notochord maturation influences myotome patterning

Because delays in notochord maturation disrupt myotome patterning (Pagnon-Minot et al., 2008), we examined slow and medial fast muscle specification in Fstl1/2 morphant embryos. During early somitogenesis stages, Hedgehog (Hh) activity maintains *myod1* expression in slow and medial fast muscle precursors (Barresi et al., 2000; Linker et al., 2003; Wolff et al., 2003). In embryos lacking Fstl1/2, *myod1* expression was upregulated in the presumptive slow and medial fast territories of the somite (see Fig. S7A,B in the supplementary material). Immunostaining with antibodies against Myod1 confirmed a significant increase in Myod1-positive cells when compared with controls (see Fig. S7 in the supplementary material) (74.6 versus 120.4, n=5; P<0.001). Fstl1/2 morphant embryos also displayed an increase in horizontal myoseptum size, as evidenced by immunostaining with F59 antibodies that

recognize mainly slow muscle (see Fig. S7G,H in the supplementary material) (Devoto et al., 1996). Likewise, the number of Engrailed-positive cells, which are induced in response to Hh activity (Wolff et al., 2003), was increased in Fstl1/2 morphants (see Fig. S7J,K,M,N in the supplementary material).

Attenuation of BMP activity at 80% epiboly had the converse effect on myofiber specification. Although *myod1* expression was maintained in presumptive slow muscle cells in *tBR* embryos, a significantly smaller number of Myod1-positive cells were found in the presumptive medial fast muscle domain (see Fig. S7C,F in the supplementary material) (57.2 versus 74.6, n=5; P<0.001). Embryos failed to form an organized horizontal myoseptum, and exhibited a reduction in Engrailed-positive muscle pioneers and medial fast muscle fibers (see Fig. S7I,L,O in the supplementary material). The disruptions in myofiber specification suggest that the timing of notochord maturation influences Hh activity levels in adjacent paraxial mesoderm.

DISCUSSION

Members of the BMP family of signaling molecules are typically assigned roles in specification of ventral cell fate. Here, we describe a previously unappreciated function for BMP signaling in the promotion of dorsal fate. We demonstrate that Bmp4 patterns axial tissue by promoting chordamesoderm proliferation, ultimately influencing the size of the notochord and CNH. Two BMP antagonists, Fstl1 and Fstl2, modulate BMP activity to appropriate levels in chordamesoderm. In their absence, the chordamesoderm domain is expanded, and these cells do not transition into mature notochord in a timely manner. Conversely, in the absence of Bmp4 the chordamesodermal domain shrinks and notochord cells differentiate prematurely. As such, we demonstrate a requirement for BMP activity in the timing of notochord differentiation.

Axial requirements for BMP activity change as gastrulation proceeds

Models addressing BMP activity in embryogenesis have established the ventralizing role of BMP signaling in specifying DV fate (Kimelman, 2006; Schier and Talbot, 2005). Surprisingly, our study demonstrates a dynamic requirement of axial tissue for BMP activity during gastrulation. Following establishment of the DV axis, axial cells require tightly regulated levels of BMP activity for proper patterning of chordamesoderm and its precursor pool. Changes in axial requirements for BMP activity are consistent with two recent studies in zebrafish examining BMP and Nodal activity during zebrafish gastrulation. Tucker and colleagues (Tucker et al., 2008) demonstrated that BMP patterning of the DV axis occurs progressively in an anterior to posterior fashion as gastrulation proceeds. Hagos and Dougan (Hagos and Dougan, 2007) demonstrated that cells responsive to Nodal signaling acquire their fate based upon the cumulative dose of Nodal signals the cell receives. This is a function of both the competence of the receiving cells as well as the strength of the signal. These studies suggest that cells possess different requirements for activity gradients as gastrulation proceeds. This is in agreement with the characteristic migration of two margins into proximity with the other during gastrulation: the ventral margin secreting BMP ligands and the dorsal organizer secreting BMP antagonists (Agathon et al., 2003). As the circumference of the margins decrease during epiboly, cells populating ventral and dorsal margins receive increasing amounts of factors secreted from the other margin. The question is, at what point does distance between the two margins influence the BMP activity gradient on the dorsal side of the gastrula?

Our results demonstrate that the ventral margin does indeed influence cells arising from the dorsal margin, beginning during the transition from mid- to late-gastrulation. Attenuation of total BMP activity at any developmental stage between 80% epiboly and the 3-somite stage arrests chordamesodermal proliferation, culminating in a reduction in the size of the notochord and CNH. Because attenuation of BMP activity after the 3-somite stage has no apparent effect

on axial structures, we propose that BMP ligands emanating from the ventral organizer during late gastrulation signal presumptive axial cells in the dorsal margin.

It is possible, although unlikely, that axial cells require BMP activity prior to late gastrulation. Labeling embryos with PSMAD1/5/8 antibodies at hourly intervals has revealed that PSMAD1/5/8-positive cells are not observed in the dorsal gastrula until late gastrulation (Tucker et al., 2008). Therefore, the rise of PSMAD1/5/8 levels after 80% epiboly in Fstl1/2 morphants is consistent with a role in mediating BMP activity in axial tissue.

Selective requirement of BMP activity in the chordamesoderm

Nodal activity is crucial for both the induction of mesoderm and the specification of axial cell fate (Kimelman, 2006; Schier and Talbot, 2005; Stemple, 2005). The location of cells within the dorsal organizer dictates the level of Nodal activity that axial mesoderm receives. High levels of Nodal signaling specify deep *gsc*-expressing prechordal plate, whereas lower levels specify more superficial *flh*-expressing chordamesoderm (Gritsman et al., 2000; Saude et al., 2000). As Follistatin binds Activin ligands (Harrington et al., 2006; Nakamura et al., 1991), one possibility for the notochord phenotype observed in Fstl1/2 morphants is an alteration in Nodal activity. If this activity were significantly altered, one would expect a transfating between types of axial mesoderm, as has been observed in mutants lacking zygotic contribution of the Nodal co-receptor Oep (Gritsman et al., 2000). However, we observe no changes in the prechordal domain of Fstl1/2 morphants, as assayed by the expression of the Nodal-responsive gene *gsc* and PSMAD2 levels. Furthermore, the phenotypes observed in chordamesoderm and notochord of embryos with reduced BMP activity are complementary to those observed in Fstl1/2 morphants. Thus, the main role of Fstl1/2 is to modulate BMP activity.

Two models can explain the inability of prechordal cells to respond to BMP signaling: the location of these cells during gastrulation, or their competence to respond to Bmp4. As gastrulation proceeds, prechordal plate cells rapidly increase their distance from the ventral margin, distancing themselves from BMP-secreting cells. If prechordal cells were competent to respond to Bmp4, *gsc* expression would be altered in embryos receiving Bmp4-soaked beads. Therefore, a more plausible model is that prechordal plate cells are not competent to respond to Bmp4 during mid- to late-gastrulation, which would make them distinct from chordamesoderm precursors in the dorsal organizer.

A balance between proliferation of the CNH and differentiation of chordamesoderm

Our results indicate that during late gastrulation through early somitogenesis, BMP signaling regulates the size of the chordamesodermal domain by establishing its proliferative state. In the absence of Bmp4, chordamesodermal cells prematurely transition into differentiated notochord. Conversely, chordamesodermal proliferation is increased in Fstl1/2 morphants and maturation of the notochord is delayed. BMP signaling may play a dual independent role to control the proliferative status of the CNH and chordamesoderm and to regulate the timely differentiation of notochord precursors. By inhibiting cell proliferation over the same window at which BMP activity influences the proliferative state of chordamesoderm, we were able to mimic the notochord phenotype observed in *tBR* embryos and Bmp4 morphants. Additionally, blocking cell proliferation inhibits the prolonged maintenance of chordamesodermal character observed in Fstl1/2 morphants. As heat-shocking *tBR* embryos after the 3-somite stage has no apparent effect on indicators of notochord differentiation, it is likely that BMP activity does not directly delay chordamesoderm maturation. Rather, the evidence presented suggests a single role for BMP signaling in controlling proliferation and favors a causal link between CNH proliferation and notochord maturation. We propose a model where the size of the axial precursor pool, established by Bmp4 and tightly controlled by two Fstl proteins, ultimately determines the maturation schedule of the notochord. Although we demonstrate the

requirement of Fstl1 and Fstl2 in this process, both *chordin* (*chd*) and *noggin1/2* (*nog1/2*) are also chordamesodermally expressed, with *nog1/2* expression persisting in the CNH through notochord maturation (Furthauer et al., 1999; Miller-Bertoglio et al., 1997). Although their requirement in DV specification prevents simple morpholino-mediated inactivation (Dal-Pra et al., 2006; Hammerschmidt et al., 1996a; Hammerschmidt et al., 1996b; Schulte-Merker et al., 1997), we cannot rule out that either *chd* or *nog1/2* might act synergistically with *fstl1/2* in chordamesoderm development as they do in early DV patterning. Similar models for a role of Bmp4 signaling in balancing proliferation and differentiation have been proposed in other contexts. The influence Bmp4 exerts over hematopoietic stem cell (HSC) proliferation (Zhang and Li, 2005) draws parallels with the effect of losing Bmp4 on the CNH. Bmp4 promotes the proliferative state of HSCs while delaying differentiation (Zhang et al., 2003). In the absence of Bmp4, HSCs exit the cell cycle and differentiate prematurely (Bhatia et al., 1999).

In addition to notochord contributions, cells from the CNH give rise to floor plate and tailbud mesoderm (Cambray and Wilson, 2002; Charrier et al., 1999; Davis and Kirschner, 2000). Our transplantation experiments suggest a particular requirement for BMP responsiveness in chordamesoderm: BMP-responsive cells preferentially populate the notochord, whereas cells unresponsive to BMP signaling contribute to paraxial and tailbud mesoderm. In addition to its role in proliferation and differentiation, differential levels of BMP activity appear to be crucial in relegating CNH cells to a particular fate.

Experiments by Agathon and colleagues (Agathon et al., 2003) have shown that the BMP-rich ventral margin in zebrafish posses tail organizer activity that contributes to non-axial derivatives in the tail, whereas the CNH, which is derived from the dorsal organizer, contributes to axial components. Their data, along with other studies (Beck et al., 2001; Gont et al., 1993; Pyati et al., 2005; Tucker and Slack, 1995) suggest that axial and non-axial tissues of the tailbud can develop independently under certain experimental conditions. However, as these two organizing centers move into close proximity at the end of gastrulation, they probably need to interact with each other to promote the coordinated growth, patterning and differentiation of the tailbud. Our studies have revealed a requirement for BMP signaling from the ventral margin on the dorsal organizer, providing a mechanism by which such coordination can be achieved and demonstrating previously unappreciated roles of BMP activity in the patterning and maturation of axial structures.

Supplementary Material

Refer to Web version on PubMed Central for supplementary material.

Acknowledgments

We thank M. Halpern for comments and criticisms on the manuscript, D. Kimelman and U. Pyati for the *Tg (hsp70l:dnBmpr-GFP)w30* zebrafish line and M. Esterberg for assistance with statistics. The F59 and 4D9 antibodies developed by F. Stockdale and C. Goodman, respectively, were obtained from the Developmental Studies Hybridoma Bank developed under the auspices of the NICHD and maintained by The University of Iowa, Department of Biology, Iowa City, IA 52242. This work was supported by an NIH grant to A.F. (DC004701).

References

Agathon A, Thisse C, Thisse B. The molecular nature of the zebrafish tail organizer. Nature 2003;424:448–452. [PubMed: 12879074]

Barresi MJ, Stickney HL, Devoto SH. The zebrafish slow-muscle-omitted gene product is required for Hedgehog signal transduction and the development of slow muscle identity. Development 2000;127:2189–2199. [PubMed: 10769242]

Bauer H, Meier A, Hild M, Stachel S, Economides A, Hazelett D, Harland RM, Hammerschmidt M. Follistatin and noggin are excluded from the zebrafish organizer. Dev. Biol 1998;204:488–507. [PubMed: 9882485]

Beck CW, Whitman M, Slack JM. The role of BMP signaling in outgrowth and patterning of the Xenopus tail bud. Dev. Biol 2001;238:303–314. [PubMed: 11784012]

Bhatia M, Bonnet D, Wu D, Murdoch B, Wrana J, Gallacher L, Dick JE. Bone morphogenetic proteins regulate the developmental program of human hematopoietic stem cells. J. Exp. Med 1999;189:1139–1148. [PubMed: 10190905]

Cambray N, Wilson V. Axial progenitors with extensive potency are localised to the mouse chordoneural hinge. Development 2002;129:4855–4866. [PubMed: 12361976]

Cambray N, Wilson V. Two distinct sources for a population of maturing axial progenitors. Development 2007;134:2829–2840. [PubMed: 17611225]

Charrier JB, Teillet MA, Lapointe F, Le Douarin NM. Defining subregions of Hensen's node essential for caudalward movement, midline development and cell survival. Development 1999;126:4771–4783. [PubMed: 10518494]

Chocron S, Verhoeven MC, Rentzsch F, Hammerschmidt M, Bakkers J. Zebrafish Bmp4 regulates left-right asymmetry at two distinct developmental time points. Dev. Biol 2007;305:577–588. [PubMed: 17395172]

Currie PD, Ingham PW. Induction of a specific muscle cell type by a hedgehog-like protein in zebrafish. Nature 1996;382:452–455. [PubMed: 8684485]

Dal-Pra S, Furthauer M, Van-Celst J, Thisse B, Thisse C. Noggin1 and Follistatin-like2 function redundantly to Chordin to antagonize BMP activity. Dev. Biol 2006;298:514–526. [PubMed: 16890217]

Davis RL, Kirschner MW. The fate of cells in the tailbud of Xenopus laevis. Development 2000;127:255–267. [PubMed: 10603344]

Devoto SH, Melancon E, Eisen JS, Westerfield M. Identification of separate slow and fast muscle precursor cells *in vivo*, prior to somite formation. Development 1996;122:3371–3380. [PubMed: 8951054]

Dickmeis T, Rastegar S, Aanstad P, Clark M, Fischer N, Korzh V, Strahle U. Expression of the anti-dorsalizing morphogenetic protein gene in the zebrafish embryo. Dev. Genes Evol 2001;211:568–572. [PubMed: 11862464]

Dosch R, Niehrs C. Requirement for anti-dorsalizing morphogenetic protein in organizer patterning. Mech. Dev 2000;90:195–203. [PubMed: 10640703]

Fainsod A, Deissler K, Yelin R, Marom K, Epstein M, Pillemer G, Steinbeisser H, Blum M. The dorsalizing and neural inducing gene follistatin is an antagonist of BMP-4. Mech. Dev 1997;63:39–50. [PubMed: 9178255]

Furthauer M, Thisse B, Thisse C. Three different noggin genes antagonize the activity of bone morphogenetic proteins in the zebrafish embryo. Dev. Biol 1999;214:181–196. [PubMed: 10491267]

Gont LK, Steinbeisser H, Blumberg B, de Robertis EM. Tail formation as a continuation of gastrulation: the multiple cell populations of the Xenopus tailbud derive from the late blastopore lip. Development 1993;119:991–1004. [PubMed: 7916680]

Griffin KJ, Amacher SL, Kimmel CB, Kimelman D. Molecular identification of spadetail: regulation of zebrafish trunk and tail mesoderm formation by T-box genes. Development 1998;125:3379–3388. [PubMed: 9693141]

Gritsman K, Talbot WS, Schier AF. Nodal signaling patterns the organizer. Development 2000;127:921–932. [PubMed: 10662632]

Hagos EG, Dougan ST. Time-dependent patterning of the mesoderm and endoderm by Nodal signals in zebrafish. BMC Dev. Biol 2007;7:22. [PubMed: 17391517]

Halpern ME, Thisse C, Ho RK, Thisse B, Riggleman B, Trevarrow B, Weinberg ES, Postlethwait JH, Kimmel CB. Cell-autonomous shift from axial to paraxial mesodermal development in zebrafish floating head mutants. Development 1995;121:4257–4264. [PubMed: 8575325]

Hammerschmidt M, Pelegri F, Mullins MC, Kane DA, van Eeden FJ, Granato M, Brand M, Furutani-Seiki M, Haffter P, Heisenberg CP, et al. dino and mercedes, two genes regulating dorsal development in the zebrafish embryo. Development 1996a;123:95–102. [PubMed: 9007232]

Hammerschmidt M, Serbedzija GN, McMahon AP. Genetic analysis of dorsoventral pattern formation in the zebrafish: requirement of a BMP-like ventralizing activity and its dorsal repressor. Genes Dev 1996b;10:2452–2461. [PubMed: 8843197]

Hammond CL, Hinits Y, Osborn DP, Minchin JE, Tettamanti G, Hughes SM. Signals and myogenic regulatory factors restrict pax3 and pax7 expression to dermomyotome-like tissue in zebrafish. Dev. Biol 2007;302:504–521. [PubMed: 17094960]

Harrington AE, Morris-Triggs SA, Ruotolo BT, Robinson CV, Ohnuma S, Hyvonen M. Structural basis for the inhibition of activin signalling by follistatin. EMBO J 2006;25:1035–1045. [PubMed: 16482217]

Holley SA. Anterior-posterior differences in vertebrate segments: specification of trunk and tail somites in the zebrafish blastula. Genes Dev 2006;20:1831–1837. [PubMed: 16847343]

Iemura S, Yamamoto TS, Takagi C, Uchiyama H, Natsume T, Shimasaki S, Sugino H, Ueno N. Direct binding of follistatin to a complex of bone-morphogenetic protein and its receptor inhibits ventral and epidermal cell fates in early Xenopus embryo. Proc. Natl. Acad. Sci. USA 1998;95:9337–9342. [PubMed: 9689081]

Imai Y, Gates MA, Melby AE, Kimelman D, Schier AF, Talbot WS. The homeobox genes vox and vent are redundant repressors of dorsal fates in zebrafish. Development 2001;128:2407–2420. [PubMed: 11493559]

Joly JS, Joly C, Schulte-Merker S, Boulekbache H, Condamine H. The ventral and posterior expression of the zebrafish homeobox gene eve1 is perturbed in dorsalized and mutant embryos. Development 1993;119:1261–1275. [PubMed: 7905819]

Kanki JP, Ho RK. The development of the posterior body in zebrafish. Development 1997;124:881–893. [PubMed: 9043069]

Kawahara A, Wilm T, Solnica-Krezel L, Dawid IB. Antagonistic role of vega1 and bozozok/dharma homeobox genes in organizer formation. Proc. Natl. Acad. Sci. USA 2000;97:12121–12126. [PubMed: 11050240]

Kimelman D. Mesoderm induction: from caps to chips. Nat. Rev. Genet 2006;7:360–372. [PubMed: 16619051]

Kitisin K, Saha T, Blake T, Golestaneh N, Deng M, Kim C, Tang Y, Shetty K, Mishra B, Mishra L. Tgf-Beta signaling in development. Sci. STKE 2007. 2007cm1.

Krauss S, Concordet JP, Ingham PW. A functionally conserved homolog of the Drosophila segment polarity gene hh is expressed in tissues with polarizing activity in zebrafish embryos. Cell 1993;75:1431–1444. [PubMed: 8269519]

Lele Z, Nowak M, Hammerschmidt M. Zebrafish admp is required to restrict the size of the organizer and to promote posterior and ventral development. Dev. Dyn 2001;222:681–687. [PubMed: 11748836]

Linker C, Lesbros C, Stark MR, Marcelle C. Intrinsic signals regulate the initial steps of myogenesis in vertebrates. Development 2003;130:4797–4807. [PubMed: 12917295]

Melby AE, Beach C, Mullins M, Kimelman D. Patterning the early zebrafish by the opposing actions of bozozok and vox/vent. Dev. Biol 2000;224:275–285. [PubMed: 10926766]

Miller-Bertoglio VE, Fisher S, Sanchez A, Mullins MC, Halpern ME. Differential regulation of chordin expression domains in mutant zebrafish. Dev. Biol 1997;192:537–550. [PubMed: 9441687]

Nakamura T, Sugino K, Titani K, Sugino H. Follistatin, an activin-binding protein, associates with heparan sulfate chains of proteoglycans on follicular granulosa cells. J. Biol. Chem 1991;266:19432–19437. [PubMed: 1918055]

Nikaido M, Tada M, Saji T, Ueno N. Conservation of BMP signaling in zebrafish mesoderm patterning. Mech. Dev 1997;61:75–88. [PubMed: 9076679]

Pagnon-Minot A, Malbouyres M, Haftek-Terreau Z, Kim HR, Sasaki T, Thisse C, Thisse B, Ingham PW, Ruggiero F, Le Guellec D. Collagen XV, a novel factor in zebrafish notochord differentiation and muscle development. Dev. Biol 2008;316:21–35. [PubMed: 18281032]

Parsons MJ, Pollard SM, Saude L, Feldman B, Coutinho P, Hirst EM, Stemple DL. Zebrafish mutants identify an essential role for laminins in notochord formation. Development 2002;129:3137–3146. [PubMed: 12070089]

Pollard SM, Parsons MJ, Kamei M, Kettleborough RN, Thomas KA, Pham VN, Bae MK, Scott A, Weinstein BM, Stemple DL. Essential and overlapping roles for laminin alpha chains in notochord and blood vessel formation. Dev. Biol 2006;289:64–76. [PubMed: 16321372]

Pyati UJ, Webb AE, Kimelman D. Transgenic zebrafish reveal stage-specific roles for Bmp signaling in ventral and posterior mesoderm development. Development 2005;132:2333–2343. [PubMed: 15829520]

Rentzsch F, Zhang J, Kramer C, Sebald W, Hammerschmidt M. Crossveinless 2 is an essential positive feedback regulator of Bmp signaling during zebrafish gastrulation. Development 2006;133:801–811. [PubMed: 16439480]

Saude L, Woolley K, Martin P, Driever W, Stemple DL. Axis-inducing activities and cell fates of the zebrafish organizer. Development 2000;127:3407–3417. [PubMed: 10903167]

Schier AF, Talbot WS. Molecular genetics of axis formation in zebrafish. Annu. Rev. Genet 2005;39:561–613. [PubMed: 16285872]

Schulte-Merker S, Ho RK, Herrmann BG, Nusslein-Volhard C. The protein product of the zebrafish homologue of the mouse T gene is expressed in nuclei of the germ ring and the notochord of the early embryo. Development 1992;116:1021–1032. [PubMed: 1295726]

Schulte-Merker S, Hammerschmidt M, Beuchle D, Cho KW, De Robertis EM, Nusslein-Volhard C. Expression of zebrafish goosecoid and no tail gene products in wild-type and mutant no tail embryos. Development 1994;120:843–852. [PubMed: 7600961]

Schulte-Merker S, Lee KJ, McMahon AP, Hammerschmidt M. The zebrafish organizer requires chordino. Nature 1997;387:862–863. [PubMed: 9202118]

Stemple DL. Structure and function of the notochord: an essential organ for chordate development. Development 2005;132:2503–2512. [PubMed: 15890825]

Stern HM, Murphey RD, Shepard JL, Amatruda JF, Straub CT, Pfaff KL, Weber G, Tallarico JA, King RW, Zon LI. Small molecules that delay S phase suppress a zebrafish bmyb mutant. Nat. Chem. Biol 2005;1:366–370. [PubMed: 16372403]

Stickney HL, Imai Y, Draper B, Moens C, Talbot WS. Zebrafish bmp4 functions during late gastrulation to specify ventroposterior cell fates. Dev. Biol 2007;310:71–84. [PubMed: 17727832]

Szeto DP, Kimelman D. The regulation of mesodermal progenitor cell commitment to somitogenesis subdivides the zebrafish body musculature into distinct domains. Genes Dev 2006;20:1923–1932. [PubMed: 16847349]

Talbot WS, Trevarrow B, Halpern ME, Melby AE, Farr G, Postlethwait JH, Jowett T, Kimmel CB, Kimelman D. A homeobox gene essential for zebrafish notochord development. Nature 1995;378:150–157. [PubMed: 7477317]

Topczewska JM, Topczewski J, Shostak A, Kume T, Solnica-Krezel L, Hogan BL. The winged helix transcription factor Foxc1a is essential for somitogenesis in zebrafish. Genes Dev 2001;15:2483–2493. [PubMed: 11562356]

Tucker AS, Slack JM. Tail bud determination in the vertebrate embryo. Curr. Biol 1995;5:807–813. [PubMed: 7583128]

Tucker JA, Mintzer KA, Mullins MC. The BMP signaling gradient patterns dorsoventral tissues in a temporally progressive manner along the anteroposterior axis. Dev. Cell 2008;14:108–119. [PubMed: 18194657]

Westerfield, M. The Zebrafish Book: A Guide for the Laboratory Use of Zebrafish. Eugene, OR: University of Oregon Press; 1994.

Willot V, Mathieu J, Lu Y, Schmid B, Sidi S, Yan YL, Postlethwait JH, Mullins M, Rosa F, Peyrieras N. Cooperative action of ADMP- and BMP-mediated pathways in regulating cell fates in the zebrafish gastrula. Dev. Biol 2002;241:59–78. [PubMed: 11784095]

Wolff C, Roy S, Ingham PW. Multiple muscle cell identities induced by distinct levels and timing of hedgehog activity in the zebrafish embryo. Curr. Biol 2003;13:1169–1181. [PubMed: 12867027]

Yamamoto Y, Oelgeschlager M. Regulation of bone morphogenetic proteins in early embryonic development. Naturwissenschaften 2004;91:519–534. [PubMed: 15517134]

Yan YL, Hatta K, Riggleman B, Postlethwait JH. Expression of a type II collagen gene in the zebrafish embryonic axis. Dev. Dyn 1995;203:363–376. [PubMed: 8589433]

Zhang J, Li L. BMP signaling and stem cell regulation. Dev. Biol 2005;284:1–11. [PubMed: 15963490]

Zhang J, Niu C, Ye L, Huang H, He X, Tong WG, Ross J, Haug J, Johnson T, Feng JQ, et al. Identification of the haematopoietic stem cell niche and control of the niche size. Nature 2003;425:836–841. [PubMed: 14574412]

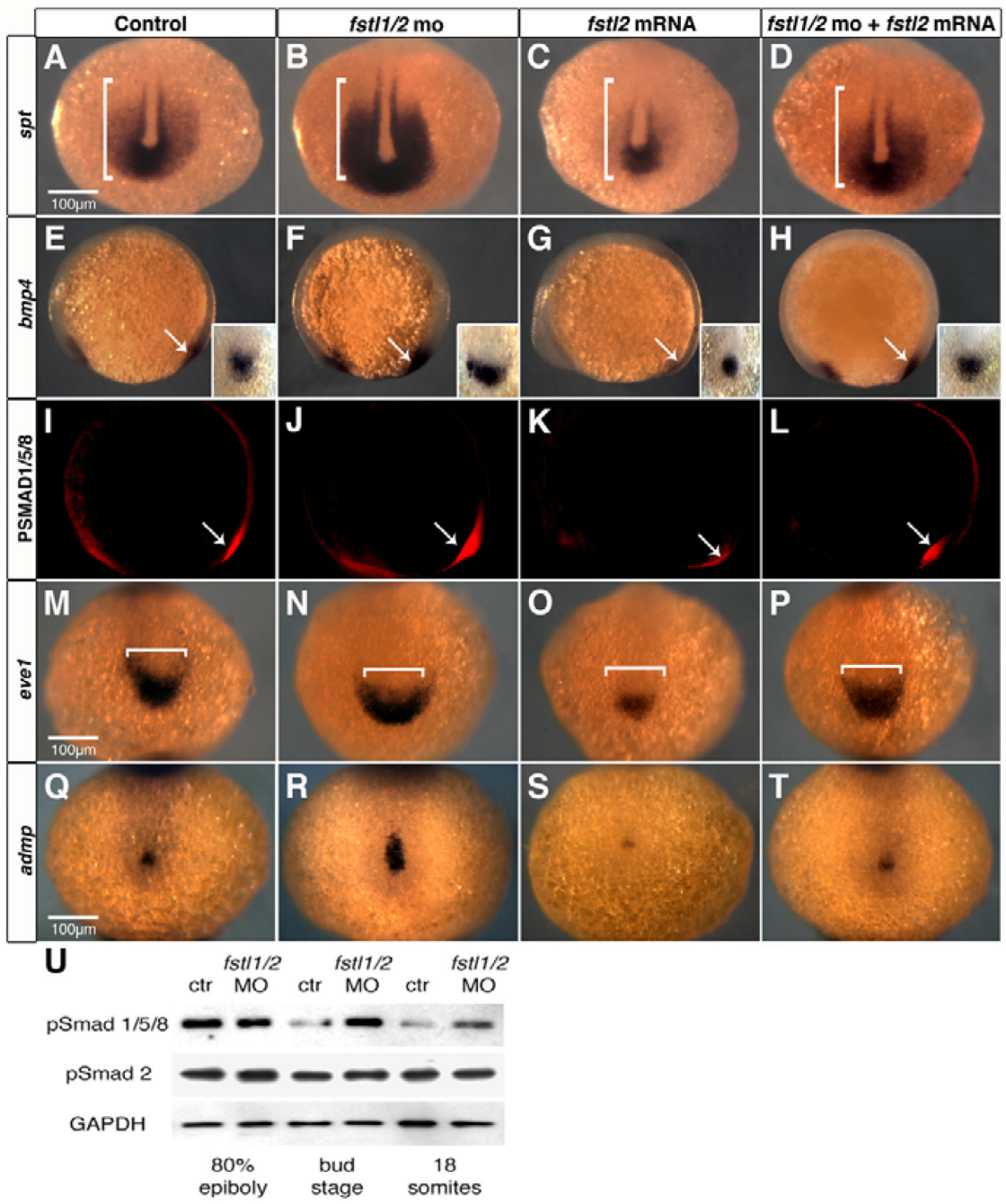

Fig. 1. Expansion of the tailbud in Fstl1/2 morphant embryos

(**A–T**) Expression of the tailbud markers *spt* (A–D), *bmp4* (E–H), PSMAD1/5/8 (I–L) and *eve1* (M–P), and the posterior axial marker *admp* (Q–T) in six-somite embryos injected with control morpholino (A,E,I,M,Q), *fstl1/2* morpholino (B,F,J,N,R), *fstl2* mRNA (C,G,K,O,S), and *fstl1/2* morpholino and *fstl2* mRNA (D,H,L,P,T). (**U**) Levels of PSMAD1/5/8, but not PSMAD2, are increased in Fstl1/2 morphants beginning at late gastrulation. All views except E–L are dorsal views, with anterior towards the top. (E–L) Lateral views, with anterior towards the left. Brackets illustrate the expression domain observed in control embryos. Arrows indicate the tailbud. Insets in E–H are views of the tailbud.

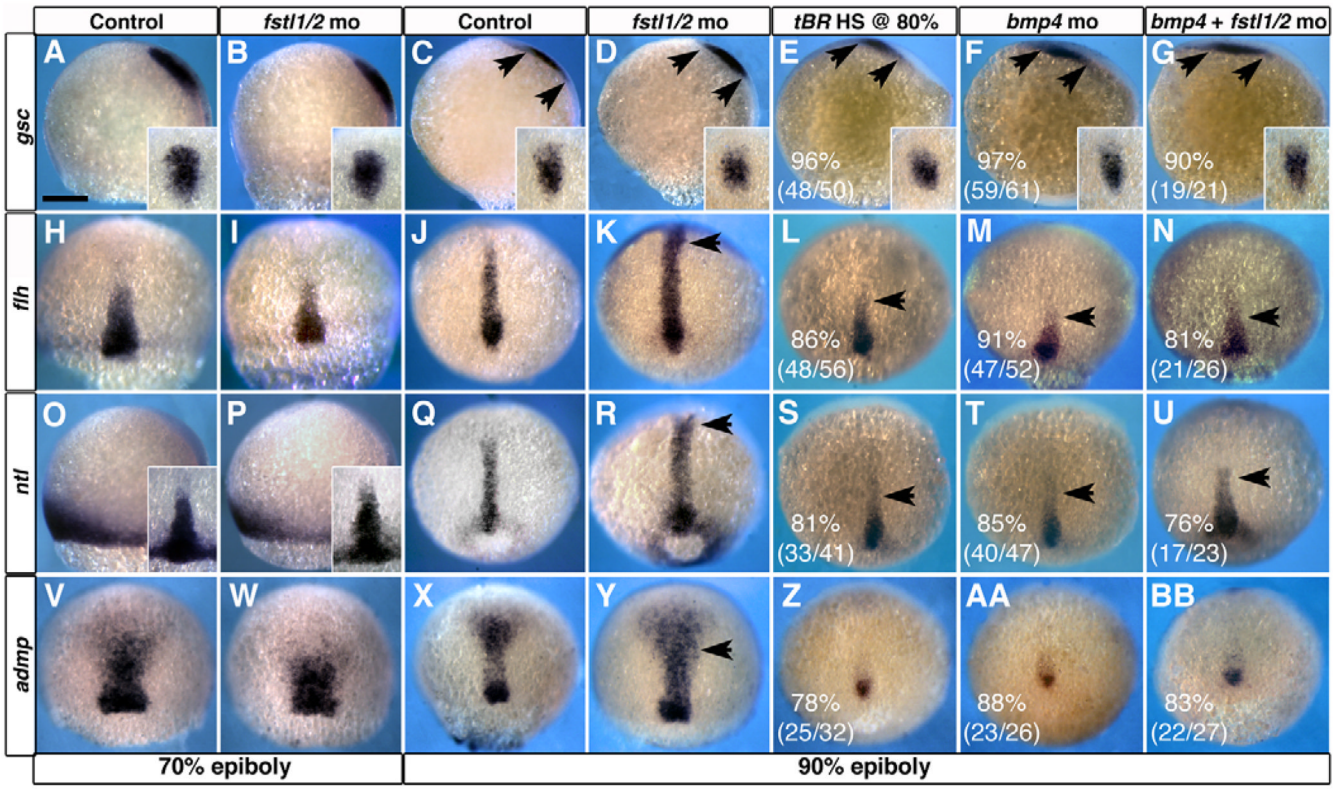

Fig. 2. Bmp4 is required in the establishment of chordamesoderm during late gastrulation

(**A**,**B**,**H**,**I**,**O**,**P**,**V**,**W**) Morpholino knockdown of Fstl1 and Fstl2 has no effect on the development of axial structures prior to 70% epiboly. (**C–F**,**J–M**,**Q–T**,**X–AA**) At 90% epiboly, alteration of BMP signaling reveals a requirement for BMP activity in patterning of chordamesoderm. (**G**,**N**,**U**,**BB**) The chordamesoderm phenotype observed when Fstl1/2 and Bmp4 are knocked down in concert resembles that of Bmp4 morphants. Arrows in C–G and K–N,R–U,Y indicate the extent of prechordal plate and chordamesoderm domains, respectively. *gsc* (C–G) expression in prechordal plate, and *flh* (J–N), *ntl* (Q–U) and *admp* (X-BB) expression in chordamesoderm. (A–G,O,P) Views are lateral, with ventral towards the left. Insets in A–G are dorsal views of the prechordal plate domain. Insets in O,P are dorsal views of chordamesodermal domain. All other views are dorsal views, with anterior towards the top. Scale bar in A: 100 μm in all panels.

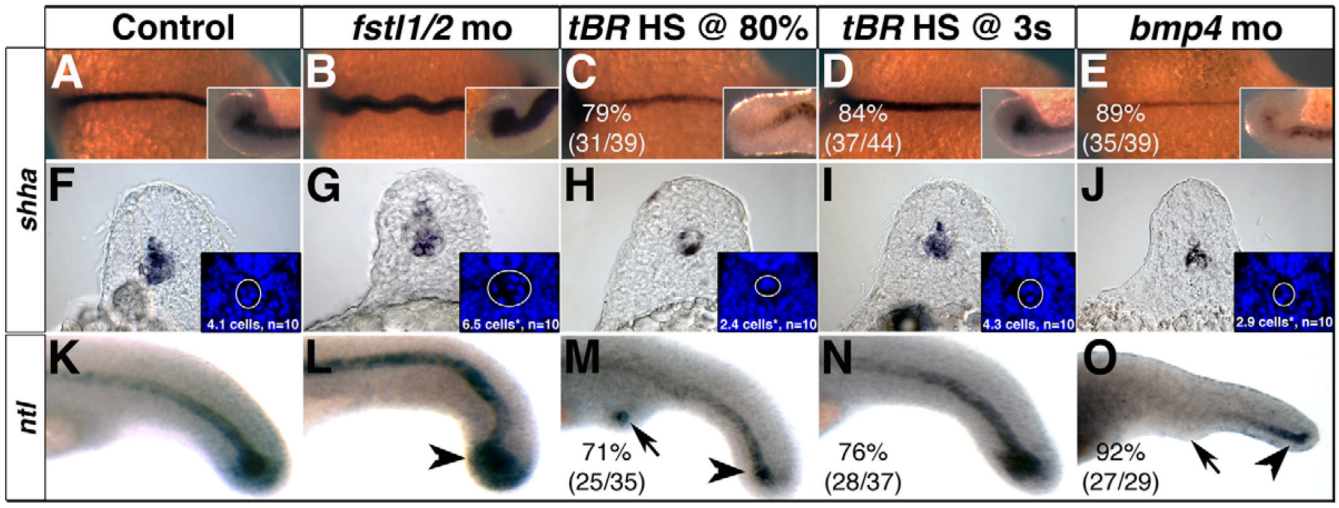

Fig. 3. Sizes of the notochord and chordoneural hinge (CNH) are influenced by Bmp4 activity during late gastrulation

(**A–E**) *shha* expression in 14-somite stage embryos. Insets are lateral views of the CNH. (**F–J**) *shha* expression in sections through somites 5–10 of 18-somite stage embryos. Insets are cropped images of the same section stained with DAPI. The mean number of DAPI-stained cells from 10 experimental embryos was subjected to one-way ANOVA, followed by a two-tailed, equal variance *t*-test. (G,H,J) Asterisks indicate significance ($P<0.001$). (**K–O**) *ntl* expression in 24 hpf embryos. CNH domains are indicated with arrowheads, arrows indicate to ectopic tail formation. (A–E) Dorsal views, with anterior towards the left. (K–O) Lateral views, with anterior towards the left.

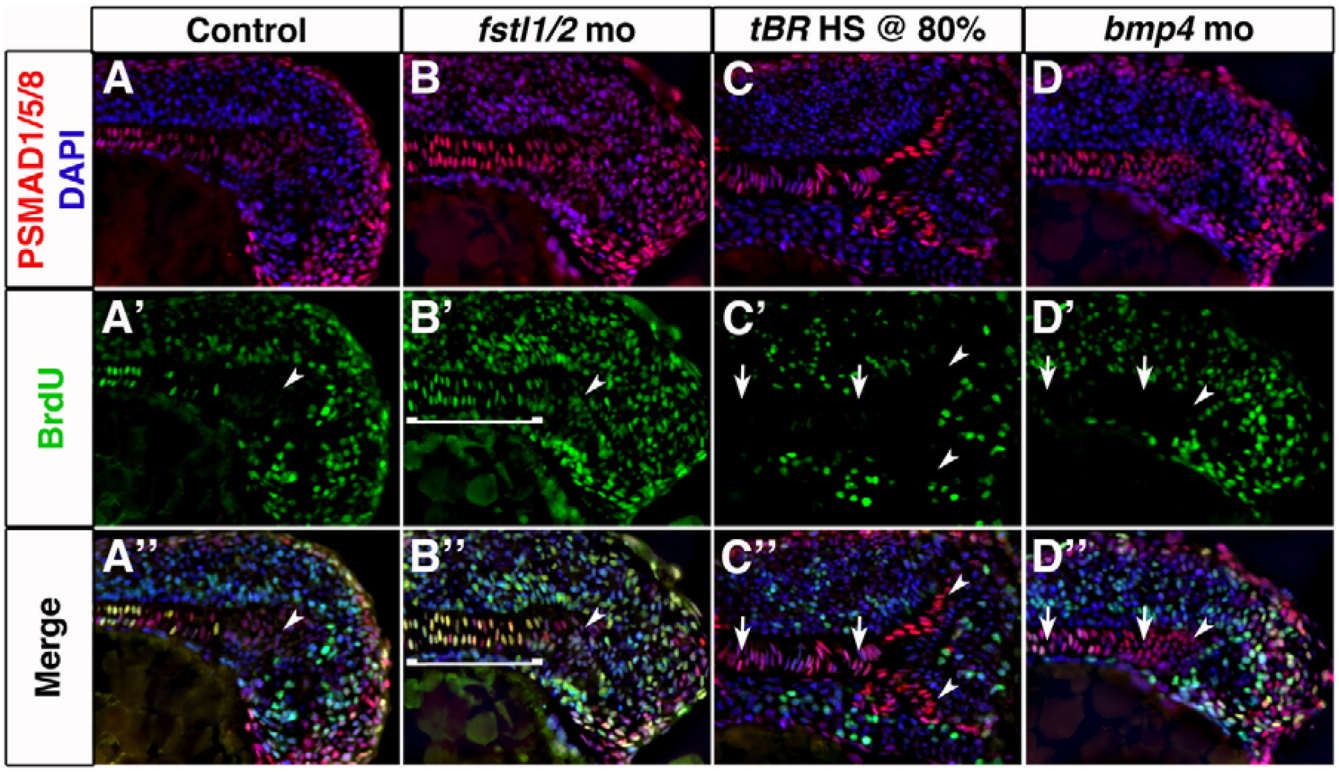

Fig. 4. BMP activity establishes proliferation in axial mesoderm

(**A–D**″) Longitudinal sections through the tailbud of 14-somite embryos exposed to PSMAD1/5/8 (red) and BrdU (green) antibodies reveal that axial cells undergoing proliferation are responding to BMP activity. Cell proliferation is increased in axial tissue of Fstl1/2 morphants (B-B″), and reduced in *tBR* embryos heat-shocked at 80% epiboly (C-C″) and Bmp4 morphants (D-D″). Arrowheads indicate the CNH. Anterior is towards the left in all views. Brackets and arrows indicate the expanse and absence of proliferation in chordamesoderm, respectively.

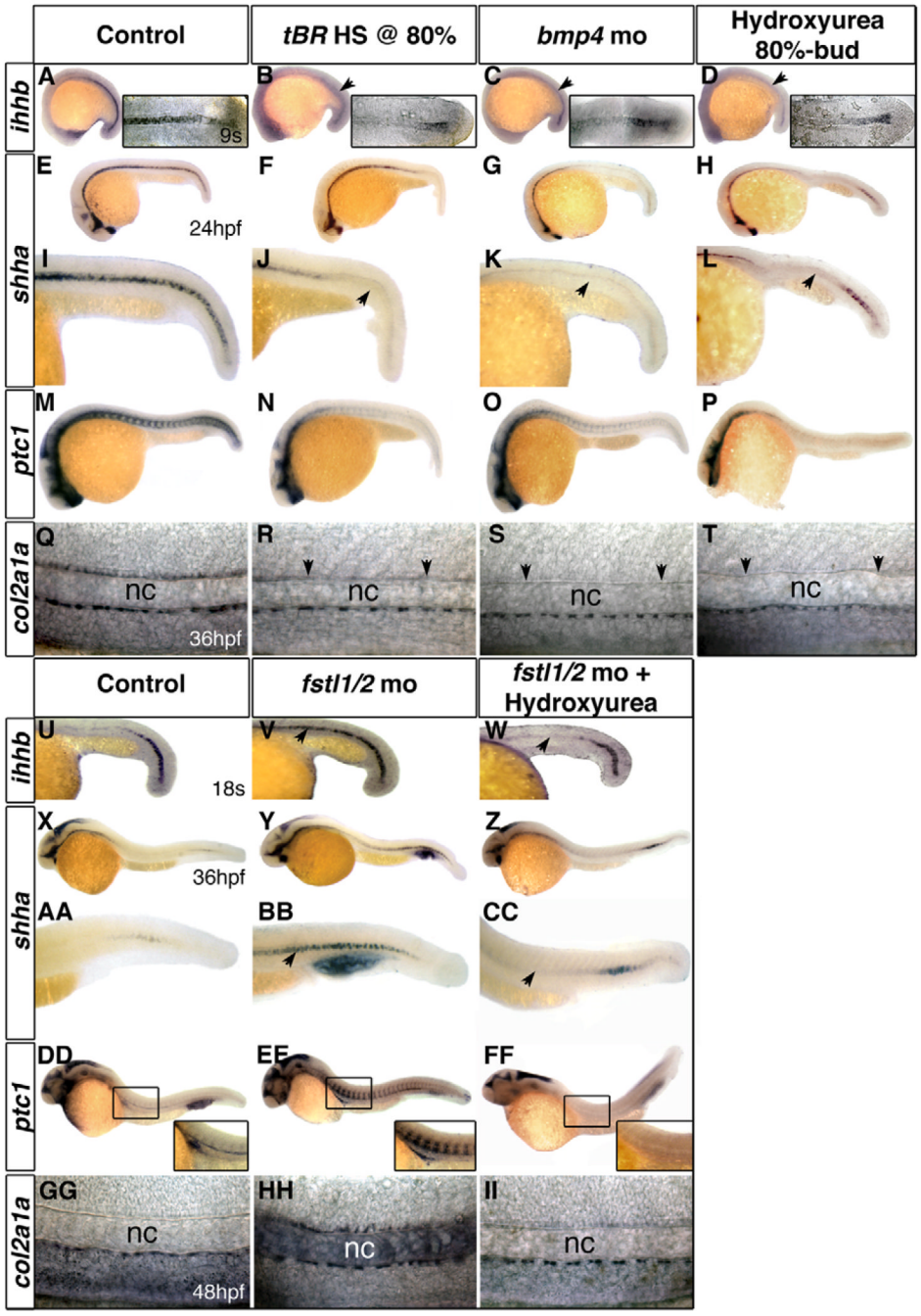

Fig. 5. The temporal state of the notochord changes with the alteration of BMP activity

The expression of chordamesoderm markers in embryos with reduced BMP activity is strongly reduced, resembling older embryos. Fstl1/2 morphant embryos maintain expression of these genes well past equivalently staged controls, resembling the expression patterns observed in younger embryos. (**A–D**,**U–W**) *ihhb* expression in 9-somite (A–D) or 18-somite stage (U–W) embryos. (**E–L**,**X-CC**) *shha* expression in 24 hpf (E–L) and 36 hpf (X-CC) embryos. (I–L,AA-CC) High-magnification view of the trunk. (**M–P**,**DD–FF**) *ptc1* expression in 24 hpf (M–P) and 36 hpf (DD–FF) embryos. (**Q–T**,**GG–II**) *col2a1a* expression in 36 hpf (Q–T) and 48 hpf (GG–II) embryos; arrows in R–T indicate absence of floorplate expression; arrows elsewhere indicate the shift in chordamesodermal gene expression relative to controls. nc, notochord. All

views are lateral, with anterior towards the left. Insets in A–D are flat-mount dorsal views. (Q–T,GG–II) Lateral views of the trunk. Insets in DD-FF indicate higher magnification views of the boxed areas.

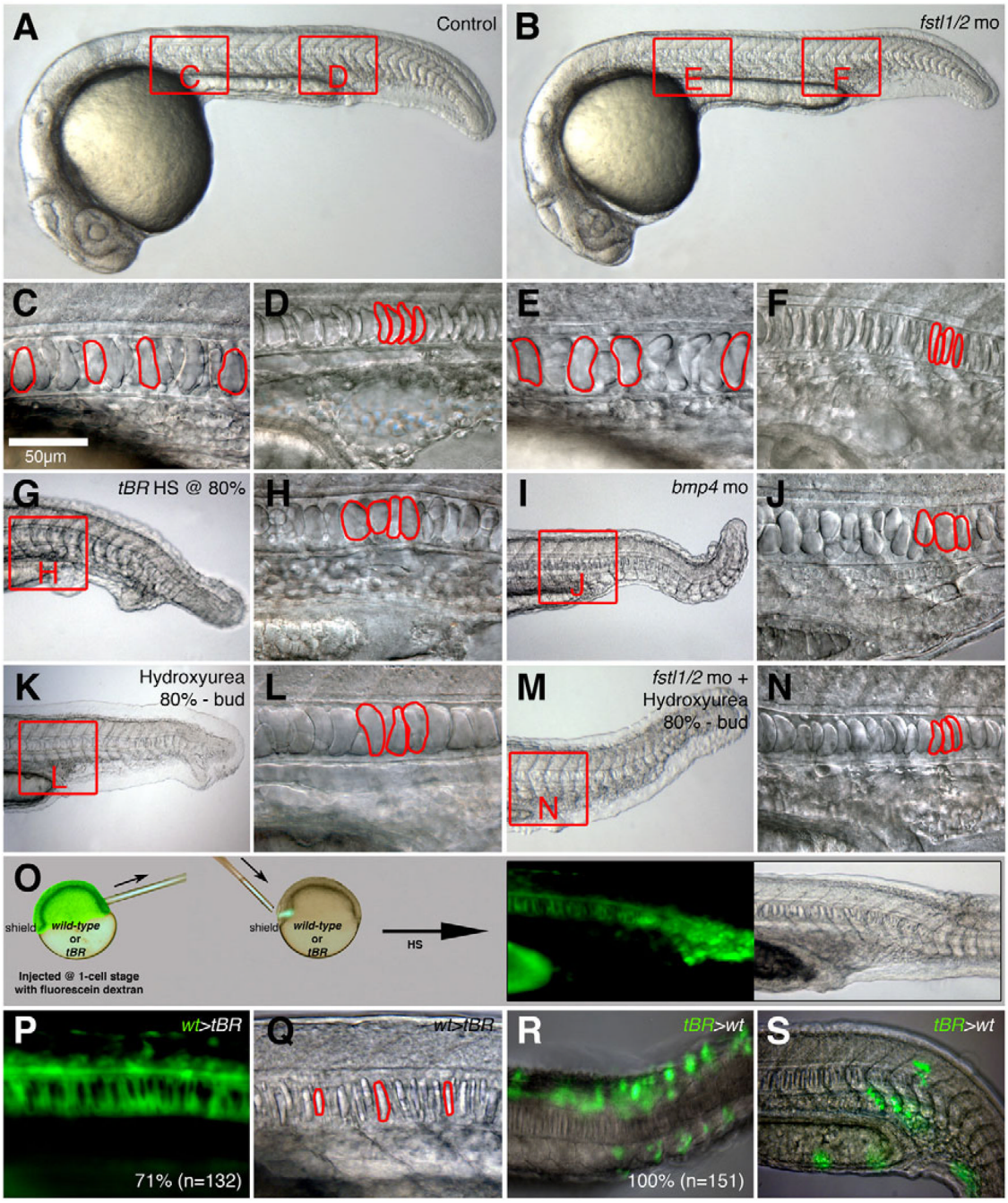

Fig. 6. Disruption of the temporal state of the notochord can be observed through notochord cell morphology

(**A**,**C**,**D**) 24 hpf control embryos; notochord cells differentiate in an anterior to posterior manner. High magnification view of notochord cells at the level of the hind yolk extension (C) and at the level of the cloaca (D). (**B**,**E**,**F**) 24 hpf Fstl1/2 morphants. High magnification view of notochord cells at the level of the hind yolk extension (E) and at the level of the cloaca (F). (**G–L**) 24 hpf *tBR* embryos heat-shocked at 80% epiboly (G,H) and Bmp4 morphants (I,J). (**K–N**) Application of cell cycle inhibitors in wild-type (K,L) and Fstl1/2 morphants (M,N). (**O**) Cell transplantation procedure. See text for details. (**P**,**Q**)Wild-type donor cells (green) populating the notochord of *tBR* embryos do not enlarge and vacuolate prematurely (Q).

(**R**,**S**) *tBR* donor cells (green) consistently fail to populate the notochord of wild-type hosts; instead, they contribute to tissues in paraxial mesoderm. All views except R are lateral views of 24 hpf embryos with anterior towards the left. (R) Dorsal view with anterior towards the left. Red outlines indicate notochord cell morphology.

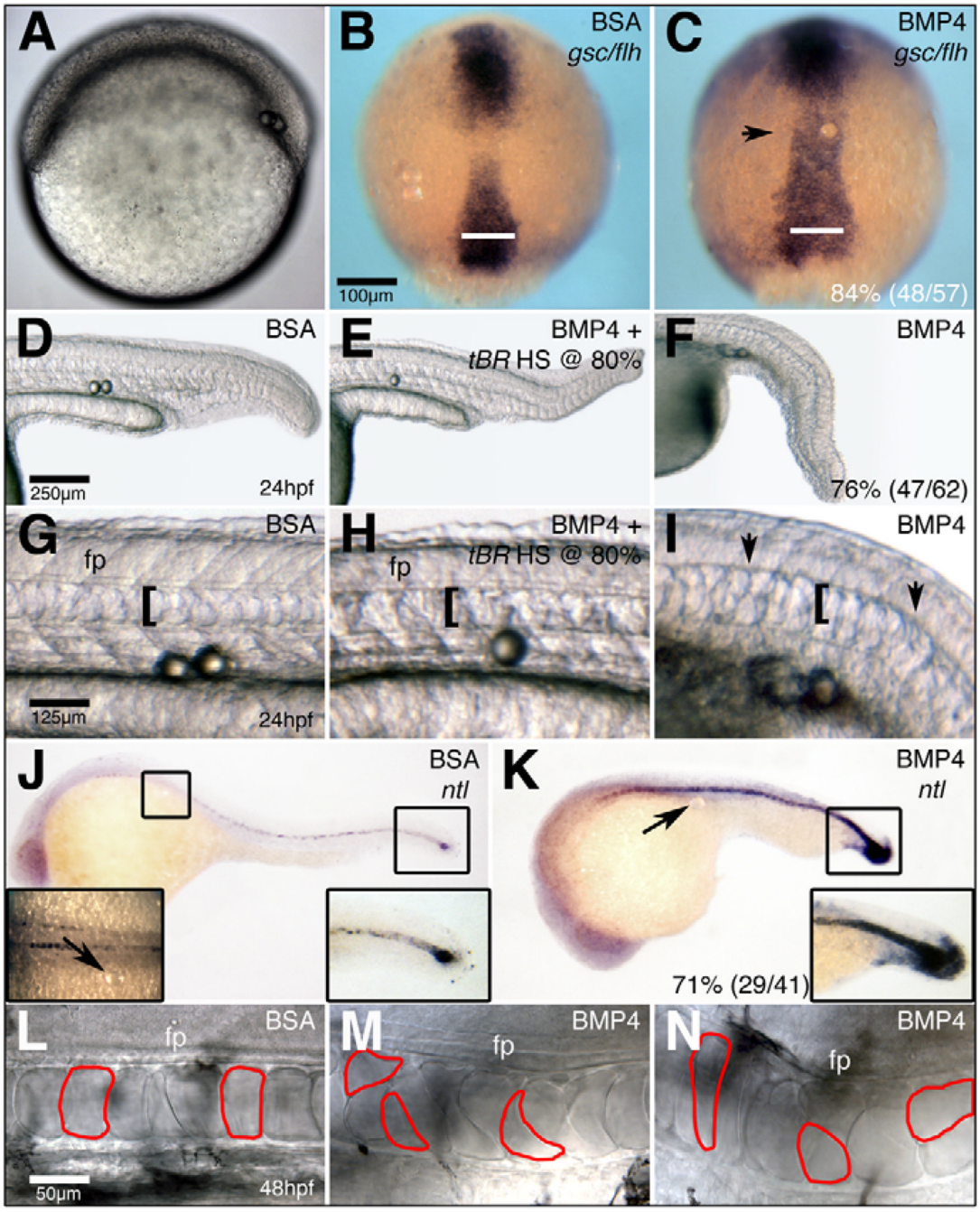

Fig. 7. A requirement for Bmp4 on the dorsal side of the gastrula

(**A**) Bead implantation on the dorsal side of the gastrula. (**B**,**C**) *gsc* and *flh* expression in 90% epiboly embryos that have had BSA- (B) or Bmp4- (C) soaked beads implanted into axial tissue. (**D**,**F**) The notochord of 24 hpf embryos implanted with BSA- (D) or Bmp4- (F) soaked beads. (**E**) *tBR* embryos implanted with Bmp4-soaked beads and heat-shocked at 80% epiboly. (**G–I**) High magnification images of the notochord in D–F. (**J**,**K**) *ntl* expression in 27 hpf embryos implanted with BSA- (J) or Bmp4- (K) soaked beads. (**L–N**) High-magnification images of the notochord at the level of the hind yolk extension of 48 hpf embryos that were implanted with BSA- (L) or Bmp4- (M,N) soaked beads. Floor plate is out of the focal plane in N. (B,C) Dorsal views, with anterior towards the top. Bars in B,C indicate the width of

chordamesodermal domain at its widest point in the control embryo in B. All other views are lateral views, with anterior towards the left. Arrows in C,J,K indicate the position of the implanted bead. Brackets and arrows in G–I indicate the width of the notochord and absence of floorplate, respectively. Red outlines in L–N indicate notochord cell morphology.